Special Issue Communications

Urban Building Height Variance From Multibaseline ERS Coherence

Adrian Luckman and William Grey

***Abstract*—Multibaseline European Remote Sensing (ERS) interferometric synthetic aperture radar coherence images from Cardiff, U.K. are investigated with respect to urban form. A model of spatial coherence, taking into account the vertical distribution of scatterers, is inverted to allow urban building height variance to be retrieved. Sixty-nine coherence maps are employed, generated from 20 ERS images. No *a priori* information is required in the analysis. However, realistic vertical scatterer distributions are retrieved, and Cardiff's central business district is automatically identified. This analysis demonstrates the utility of the urban decorrelation models employed.**

***Index Terms*—Decorrelation, interferometric synthetic aperture radar (InSAR), interferometry, surface roughness.**

I. Introduction

THE PHASE stability of anthropogenic structures between synthetic aperture radar (SAR) images has led several authors to propose long time-scale phase correlation, or coherence, as a good measure of urban extent, and thus an appropriate tool for monitoring urban change by remote sensing [1]–[3].

Coherence in urban areas is influenced by many factors including temporal delay between images, building height variance within the urban landscape, and baseline separation perpendicular to the look direction ($B_\perp$). The vertical distribution of scatterers has a strong effect in particular on the relationship between baseline and coherence [4]. This may reduce the value of coherence images in measuring urban extent when building heights are diverse and zero-baseline pairs are unavailable. However, it should also allow a measure of urban topography to be retrieved from multibaseline coherence data.

In this paper, a model of spatial decorrelation is inverted to allow scatterer height variance related to general building height to be retrieved from multibaseline coherence images. The approach is simpler than other multibaseline analyses such as tomography [5] and equally inefficient at deriving urban topography compared to other contemporary techniques such as light detection and ranging (LIDAR) [6]. However, it is valuable in validating models of decorrelation which may be important in other application areas.

II. Coherence Modeling

A. Surface Scattering Model

The degree of coherence between a pair of SAR images is an important factor in determining the quality of thematic, topographic or displacement information that can be retrieved from interferometric synthetic aperture radar (InSAR) analysis [1], [7], [8]. Hence, much theoretical work has been carried out to investigate and model the coherence between pairs of SAR images with respect to target type, baseline, surface slope and temporal delay [4], [9], [10].

Coherence is generally taken to be the product of independent factors related to the time delay between images (γ_{temporal}), the difference in signals between images due to the different positions in space from which they were acquired (γ_{spatial}) and other factors (γ_{system}). These other factors arise during data acquisition (e.g., thermal noise or differential atmospheric path delays [11]) and processing (e.g., imperfect registration of the SAR images [10]) and depend neither on repeat-pass delay nor baseline. Thus, the total observed coherence γ_{total}) is given by

$$\gamma_{\text{total}} = \gamma_{\text{temporal}} \cdot \gamma_{\text{spatial}} \cdot \gamma_{\text{system}}. \tag{1}$$

The γ_{spatial} factor is itself a product of factors related to imaging geometry and surface topography ($\gamma_{\text{slantrange}}$), and scattering mechanisms at the target, with some studies assuming a volume scattering component [12]. However, radar interactions with urban features are more likely to be of the surface scattering type (γ_{surface}) [13], and thus the baseline-dependent coherence factor in urban areas may be simplified as

$$\gamma_{\text{spatial}} = \gamma_{\text{slantrange}} \cdot \gamma_{\text{surface}}. \tag{2}$$

The $\gamma_{\text{slantrange}}$ term is given by [10] as

$$\gamma_{\text{slantrange}} = 1 - \frac{2R_s B_\perp}{\lambda r_0 |\tan(\theta_{\text{look}} - \alpha)|} \tag{3}$$

where R_s is the range resolution, $B_\perp$ is the perpendicular baseline separation, λ is the radar wavelength, θ_{look} is the look angle, r_0 is the range distance and α is the slope in the range direction.

The $\gamma_{\text{slantrange}}$ term is often compensated for by common band filtering (CBF) in which a spatial frequency filter is applied to the two images to leave only the components common between them. However, the CBF is not applied here because it is not appropriate for spatially heterogeneous targets such as urban areas [14].

If it is assumed that the ground surface slope within the urban landscape is negligible (as is the case for Cardiff), then the α term of (3) may also be considered insignificant. Further, if the variance in building height is assumed to be Gaussian distributed then γ_{surface} is given by Franceschetti *et al.* [4]

$$\gamma_{\text{surface}} = \exp\left[-\frac{1}{2}\left(\frac{4\pi h_\sigma \sin\theta_{\text{look}} B_\perp}{\lambda r_0}\right)^2\right] \tag{4}$$

where h_σ is the standard deviation in the vertical distribution of scatterers, and r_0 is the range distance.

Coherence in urban areas remains high even between images pairs separated by several years [15]. If the temporal causes of decorrelation are also assumed to be negligible, then the expected relationship between coherence and baseline for an ideal urban environment would follow the curves in Fig. 1(a).

The γ_{temporal} and γ_{system} factors are independent of baseline, should not be radically different between image pairs, and in urban areas are expected to be small compared to the baseline-dependent component. If these are considered together as γ_{other} then the total coherence model becomes

$$\gamma_{\text{total}} = \gamma_{\text{slantrange}} \cdot \gamma_{\text{surface}} \cdot \gamma_{\text{other}}. \tag{5}$$

Manuscript received September 27, 2002; revised February 12, 2003. The work of W. Grey was supported by the U.K. Natural Environment Research Council under the URGENT Programme (GST/02/2241 and GT24/98/URGE/2).

The authors are with the Department of Geography, University of Wales, SA2 8PP Swansea, U.K. (e-mail: A.Luckman@Swansea.ac.uk).

Digital Object Identifier 10.1109/TGRS.2003.815236

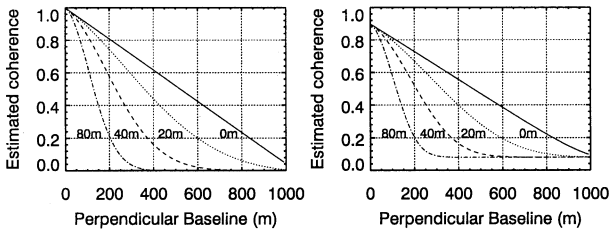

Fig. 1. Expected relationship between coherence and $B_\perp$ for a range of building height variance values (h_σ) where (a) γ_{spatial} is the only decorrelating factor, and (b) with 1×5 multilooking and using a coherence window size of 5×5 pixels and assuming a typical γ_{other} of 0.9.

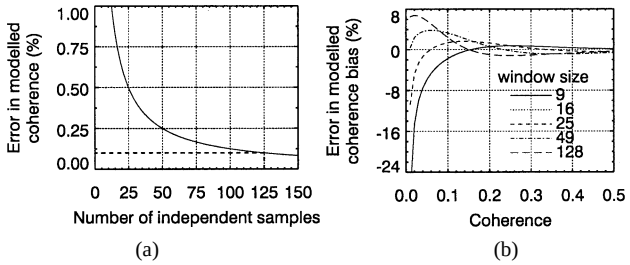

Fig. 2. Errors introduced by (a) the approximation for coherence bias when coherence is zero and (b) the overall approximate model for coherence bias.

B. Including Coherence Bias

When estimating coherence from measured image data, bias in the estimate must also be taken into account. Coherence can only be estimated from SAR imagery using finite samples. This introduces a bias in the estimate, leading to an overestimate where values are low, which is itself dependent on the coherence. To invert the model, the coherence bias must itself be modeled in such a way that it can be inverted. Coherence bias is given by Touzi and Lopes [16]

$$E[\gamma] = \frac{\Gamma(N)\Gamma(3\backslash 2)}{\Gamma(N+1\backslash 2)} {}_3F_2(3\backslash 2, N, N; N+1, 1; \gamma^2)(1-\gamma^2) \tag{6}$$

where $E[\gamma]$ is the expected value for coherence, N is the number of samples used to estimate the coherence, $\Gamma(N)$ is the gamma function of N, and ${}_3F_2$ is the hypergeometric function.

This infinite series has complex convergent properties and is therefore not straightforward to invert. However, Oliver and Quegan [17] give an approximation for the bias value where coherence is zero

$$E[\gamma_0] = \frac{\Gamma(N)\Gamma(3\backslash 2)}{\Gamma(N+1\backslash 2)} \approx \frac{1}{2}\sqrt{\frac{\pi}{N}} \tag{7}$$

where $E[\gamma_0]$ is the expected coherence when the true coherence is zero. The difference between this approximation and the full implementation of (6) is shown in Fig. 2(a). This demonstrates an error of only 0.1% for 125-look data suggesting that this approximation is valid. Thus (6) approximates to

$$E[\gamma] \approx \frac{1}{2}\sqrt{\frac{\pi}{N}} {}_3F_2(3\backslash 2, N, N; N+1, 1; \gamma^2)(1-\gamma^2). \tag{8}$$

Equation (8) is no easier to use in retrieval, but may be further approximated to an exponential function of the form

$$E[\gamma] \approx \gamma + E[\gamma_0] \exp\left(-\gamma f(N)\right) \tag{9}$$

where $f(N)$ is a simple function of the number of samples. To find $f(N)$ in this approximation, the value of coherence bias was calculated from (6) for a range of coherence values and a number of sample sizes. The value of $f(N)$ which minimized the square error between the full function and the simple function was found for each N. This varied linearly with the window size ($\sqrt{N}$), and the best fit line was found by regression

$$f(N) = 0.964\,422\sqrt{N} + 0.910\,496 \quad \text{(to six decimal places)}. \tag{10}$$

The error introduced between (6) and (9) is shown in Fig. 2(b). With 1×5 multilooking and a coherence window size of 5×5 (125 looks), the error is less than 2% for values of coherence above 0.04 (i.e., all realistic values in urban areas).

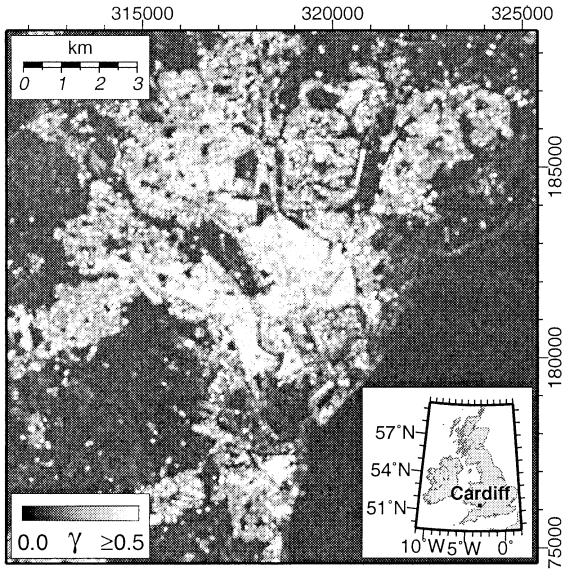

Fig. 3. Coherence image of Cardiff.

C. Fitting the Simplified Model

The retrieval model for coherence in urban areas thus becomes (constants given to two decimal places)

$$E[\gamma] \approx \gamma_{\text{total}} + \frac{1}{2}\sqrt{\frac{\pi}{N}} \exp(-(0.96\sqrt{N} + 0.91) \cdot \gamma_{\text{total}}). \tag{11}$$

Fig. 1(b) illustrates the behavior of this model with respect to baseline for a variety of surface roughness values.

Given a number of coherence measurements for different baselines from a given urban situation, it is possible to fit this model to allow the retrieval of h_σ to give an indication of the vertical distribution of scatterers and thus the aggregate difference in height between the top and bottom of buildings.

The model was fitted with h_σ and γ_{other} as free parameters so that no *a priori* information on baseline-independent decorrelation mechanisms is required. However, it is assumed that baseline-dependent mechanisms of decorrelation dominate and that there are enough measurements to form a stable fit such that differences in γ_{other} are residual.

III. Test Site and Data Processing

The city of Cardiff (Fig. 3) was chosen as a test site. SAR data from the ERS satellites were provided by the European Space Agency (ESA) and 20 images from a single descending-pass track and frame (137 and 2565, respectively) were selected from the archive.

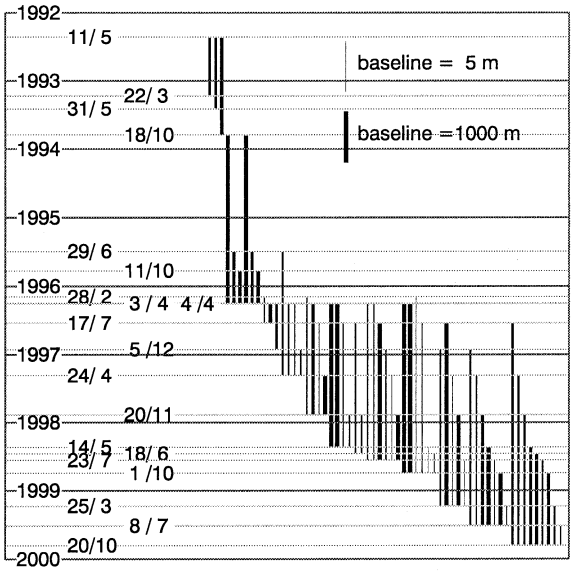

Fig. 4. Illustration of the 69 combinations of 20 ERS images used to generate coherence images along with their baselines and repeat-pass delays. The vertical length of the bars indicates repeat-pass delay and bar thickness gives an approximate indication of $B_\perp$ for each pair.

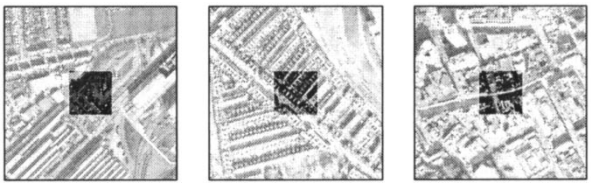

(a) (b) (c)

Fig. 5. Aerial photography of three areas of Cardiff used to validate the roughness retrieval model. (a) Parking lot. (b) Residential. (c) City center. Pixel size is 2 m and image size 400 m $\times$ 400 m. The central highlighted squares approximate the ground size of the 5 $\times$ 5 coherence window.

These 20 images allow 69 pair combinations with a good range of baselines (1 to 1000 m) where repeat-pass delays are limited to a minimum of 3 and maximum of 34 repeat-pass cycles (105 days and 3.25 years, respectively) (Fig. 4).

The first image in the time sequence was chosen as a reference and the other 19 images were coregistered to this one to subpixel accuracy. Tie-points were found automatically by cross correlation of intensity in image patches and a polynomial transformation (second order in two dimensions) was applied which typically leads to a coregistration accuracy of better than one tenth of a pixel [18].

The 69 image pair combinations were interfered using 1 $\times$ 5 multilooking (to give suitable spatial resolution with acceptable noise reduction). Coherence was estimated in 5 $\times$ 5 pixel windows to give an acceptable compromise between spatial resolution and quality of parameter retrieval. The resulting coherence images were geocoded to the British National Grid Transverse Mercator map projection with the use of a 10 m-posting digital elevation model provided by the Ordnance Survey of Great Britain.

IV. Model Testing

Three areas of Cardiff, representing low, medium, and high aggregate building heights were chosen to test the h_σ retrieval model. These were a large parking lot, residential streets, and the city center (Fig. 5).

The distribution of coherence values with respect to baseline for each coherence image of the three test areas is given in Fig. 6. The model

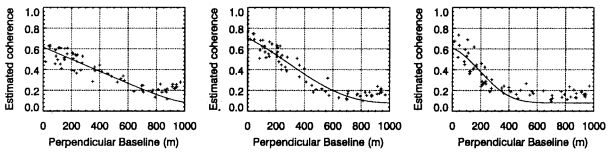

(a) (b) (c)

Fig. 6. Relationship between coherence and baseline for the three areas shown in Fig. 5. (a) Parking lot. (b) Residential. (c) City center. The simplified surface coherence model is fitted by least squares minimization giving the retrieved parameters in Table I.

TABLE I
Retrieved Values of h_σ and $\gamma_{\rm other}$ for the Example Areas Illustrated in Figs. 5 and 6

Feature	h_σ (m)	γ_{other}	RMSE
Parking lot (smooth)	0.05	0.617	0.0756
Residential area (medium)	15.6	0.705	0.0716
Cardiff city centre (rough)	35.9	0.609	0.0858

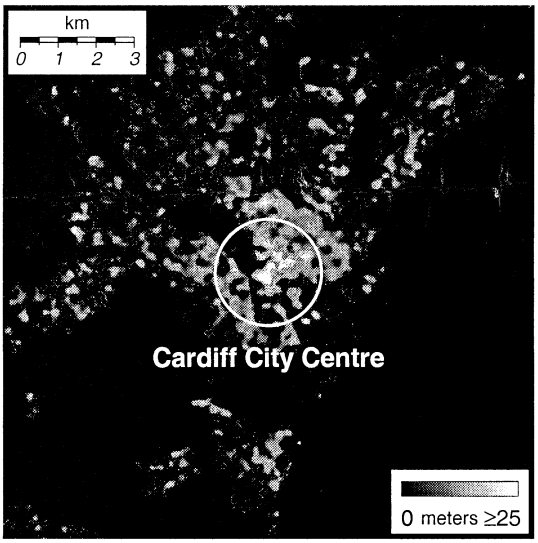

Fig. 7. Map of Cardiff building height standard deviation from multibaseline ERS interferometry. The h_σ retrieval model finds maximum building height variance in the city center.

was fitted to these data to find free parameters h_σ and $\gamma_{\rm other}$, and the root mean square error (RMSE) (Table I).

The $\gamma_{\rm other}$ term between the three examples seems to be stable, and RMSE acceptably small, suggesting that the model fit is good. Despite no *a priori* height information in the model, the retrieved value of h_σ yields realistic values. In the parking lot a value of less than 1 m is in keeping with the probable dimensions of walls and parked vehicles. In the residential area, where houses are typically 10–20 m tall, an h_σ of 15.6 m is appropriate and in the city center, which has many multistorey buildings, a value of 36 m is also in keeping with the expected vertical distribution of scatterers. The model underestimates coherence bias for large baselines because there is normally some interdependence between samples in SAR data.

V. Urban Building Variance Retrieval

The model was used to retrieve h_σ from the multibaseline coherence data in Cardiff on a full image basis. For every pixel in the images (700 $\times$ 700), the average coherence in a 9 $\times$ 9 window (to give aggregate values over an area) was found for each baseline and the two free parameters were retrieved by fitting the simplified coherence model by

least squares. The procedure was applied only to those pixels with average coherence (across the range of coherence images) above 0.5, as other areas are not believed to be representative of urban features and are therefore not appropriate for the model.

Fig. 7 shows the result of this retrieval and also indicates the location of Cardiff City center where building heights are expected to be at a maximum. The central business district of Cardiff is clearly differentiated from the rest of the city and the retrieved height variance is in keeping with the height of buildings in this area.

VI. Conclusion

By inverting a simplified coherence model, a measure of building height variance was retrieved from multibaseline ERS coherence images. The model required no *a priori* height information, yet yielded realistic building height variances and automatically identified Cardiff City center in the U.K. Whilst not as efficient as other contemporary techniques such as LIDAR, this method could be applied elsewhere to retrieve building height variance in cities on flat ground where the surrounding countryside is vegetated. Despite assumptions and approximations, the utility of the coherence models have been validated.

Acknowledgment

The authors are particularly grateful to ESA for providing ERS data through Project AO3.290. Aerial photography of Cardiff was acquired by *Cities Revealed* and provided through the NERC URGENT Programme. Thanks to Bristol and Cardiff City Councils, and Ordnance Survey for their help and advice during this project.

References

[1] T. Strozzi, P. Dammert, U. Wegmuller, J.-M. Martinez, J. Askne, A. Beaudoin, and M. Hallikainen, "Landuse mapping with ERS SAR interferometry," *IEEE Trans. Geosci. Remote Sensing*, vol. 38, pp. 766–775, Mar. 2000.

[2] S. Usai, "An analysis of the interferometric characteristics of anthropogenic features," *IEEE Trans. Geosci. Remote Sensing*, vol. 38, pp. 1491–1497, May 2000.

[3] P. Gamba, B. Houshmand, and M. Saccani, "Detection and extraction of buildings from interferometric SAR data," *IEEE Trans. Geosci. Remote Sensing*, vol. 38, pp. 611–618, Mar. 2000.

[4] G. Franceschetti, A. Iodice, M. Migliaccio, and D. Riccio, "The effect of surface scattering on IFSAR baseline decorrelation," *J. Electromagn. Waves Applicat.*, vol. 11, pp. 353–370, 1997.

[5] A. Reigber and A. Moreira, "First demonstration of airborne SAR tomography using multibasline L-band data," *IEEE Trans. Geosci. Remote Sensing*, vol. 35, pp. 2142–2152, Sept. 2000.

[6] P. Gamba and B. Houshmand, "Digital surface models and building extraction: A comparison of IFSAR and LIDAR data," *IEEE Trans. Geosci. Remote Sensing*, vol. 38, pp. 1959–1967, July 2000.

[7] R. Bamler and P. Hartl, "Synthetic aperture radar interferometry," *Inv. Prob.*, vol. 14, pp. R1–R54, 1998.

[8] F. Li and R. Goldstein, "Studies of multibaseline spaceborne interferometric synthetic aperture radars," *IEEE Trans. Geosci. Remote Sensing*, vol. 28, pp. 88–97, Jan. 1990.

[9] A. Fanelli, M. Ferri, M. Santoro, and A. Vitale, "Analysis of coherence images over urban areas in the extraction of building heights," in *Proc. IEEE/ISPRS Joint Workshop on Remote Sensing and Data Fusion Over Urban Areas*, Rome, 2001.

[10] H. Zebker and J. Villasenor, "Decorrelation in interferometric radar echoes," *IEEE Trans. Geosci. Remote Sensing*, vol. 30, pp. 950–959, Sept. 1992.

[11] H. Zebker, P. Rosen, and S. Hensley, "Atmospheric effects in interferometric synthetic aperture radar surface deformation and topographic maps," *J. Geophys. Res.—Solid Earth*, vol. 102, no. 4, pp. 7547–7563, 1987.

[12] E. Hoen and H. Zebker, "Penetration depth inferred from interferometric volume decorrelation observed over the Greenland ice sheet," *IEEE Trans. Geosci. Remote Sensing*, vol. 38, pp. 2571–2583, Nov. 2000.

[13] F. M. Henderson and Z. Xia, "SAR applications in human settlement detection, population estimation and urban land use pattern analysis: A status report," *IEEE Trans. Geosci. Remote Sensing*, vol. 35, pp. 79–85, Jan. 1997.

[14] F. Gatelli, A. M. Guarnieri, F. Parizzi, P. Pasquali, C. Prati, and F. Rocca, "The wavenumber shift in SAR interferometry," *IEEE Trans. Geosci. Remote Sensing*, vol. 32, pp. 855–865, July 1994.

[15] S. Usai and R. Klees, "SAR interferometry on a very long time scale: A study of the interferometric characteristics of man-made features," *IEEE Trans. Geosci. Remote Sensing*, vol. 37, pp. 2118–2123, July 1999.

[16] R. Touzi, A. Lopes, J. Bruniquel, and P. Vachon, "Coherence estimation for SAR imagery," *IEEE Trans. Geosci. Remote Sensing*, vol. 37, pp. 135–149, Jan. 1999.

[17] C. Oliver and S. Quegan, *Understanding Synthetic Aperture Radar Images*. Norwood, MA: Artech House, 1998.

[18] U. Wegmuller, C. L. Werner, and T. Strozzi, "SAR interferometric and differential interferometric processing chain," in *Proc. IGARSS*, Seattle, WA, 1998.